Supplementary Information

Autophagy protects against active tuberculosis by suppressing bacterial burden and inflammation

Castillo et al.

Contents: Supplementary results, supplementary materials and methods, supplementary figure legends, and supplementary figures

Supplementary results

Histopathological findings in $Atg5^{fl/fl}$ LysM-Cre^{+} mice infected with *M. tuberculosis* H37Rv

At necropsy the veterinary pathologist's findings were as follows: the Atg5-deficient mice exhibited extensive, discrete multinodular to coalescing foci of lung inflammation (granulomas), whereas the $Atg5^{fl/fl}$ LysM-Cre^{-} mice exhibited more subtle lung lesions characterized by mild, patchy foci of white discoloration without nodule formation (Figure 1C). Microscopic examination revealed that the lungs from the $Atg5^{fl/fl}$ LysM-Cre^{+} mice exhibited marked pulmonary inflammation resembling the caseating granulomas found in cases of human TB, characterized by nodular, often coalescing foci consisting of peripheral infiltrates of lymphocytes, macrophages, plasma cells and occasional neutrophils, surrounding central foci of necrotic debris containing dead and dying neutrophils (Figure 1D). Acid-fast staining of the lungs from these mice revealed abundant intracellular and extracellular bacilli. In contrast, lungs from the infected $Atg5^{fl/fl}$ LysM-Cre^{-} mice exhibited only irregular, mild to moderate, bronchoalveolar and interstitial infiltrates of lymphocytes, macrophages and plasma cells without organization into discreet nodules. Acid-fast staining of lungs from these mice revealed very sparse intracellular bacilli, and no apparent extracellular bacilli (Figure 1D).

Supplementary Materials and Methods

***M. tuberculosis* infection of $Atg5^{fl/fl}$ LysM-Cre mice.** *M. tuberculosis*, strain H37Rv, inoculum was prepared by diluting a frozen stock of known titer in sterile PBS/0.05% Tween 80. Mice were anesthetized with isofluorane (Abbott Laboratories, Chicago, IL) and 50 µl of fluid containing *M. tuberculosis* were placed on the nostrils of mice, after which mice were allowed to inhale the inoculum under direct observation. The mice awoke approximately 1 minute after sedation. The mice were kept warm with a heat lamp and allowed to recover under direct observation. One hour after inoculation, 3 randomly selected mice from the infected cohort were harvested to determine lung depositions. Bacterial burden was determined using homogenized organs. Samples were serially diluted and duplicated, and 50 µl aliquots of each dilution were spread on Selective Mitchinson 7H11 agar plates (Remel) and placed into humidified incubator at 37°C for 12 days.

Mice were weighted twice prior to infection on days -3 and -1 for baseline. Upon infection, mice were monitored daily for survival and weighted semi-weekly. At the indicated times, mice were sacrificed by CO_2 overdose, and lungs were harvested and homogenized in 1 ml of PBS/0.05% Tween 80. For histopathological examination, lungs were insufflated with 10% neutral buffered formalin via tracheal cannulation and removed *en bloc*. At the same time, spleens were harvested and all organs were placed into 10% buffered formalin for further processing in histological studies. Paraffin-embedded sections were stained with hematoxylin and eosin (H&E stain) or acid fast stain and evaluated by a board certified veterinary pathologist. Samples were subjected to a freeze/thaw cycle, sonicated for 30 sec, allowed to sit on ice for 30 min, centrifuged at 12,000 rpm for 10 min, supernatants collected and filtered through a 0.45 µm syringe filter and assayed for cytokines using the Luminex Multiplex System (Luminex Corp, Austin TX). Beads for cytokine quantification were from Invitrogen and used according to the manufacturer's instruction.

Cells and tissue preparation. Lungs were perfused with sterile saline in order to remove peripheral blood cells. Lungs were then minced and enzymatically (DNAse/collagenase solution) treated at 37^{o} C for 60 min. The digested lung tissue was then mechanically disrupted using a pestle and wire screen. Cells were then filtered over a nylon wool column to remove particulate and remaining red blood cells were lysed and cells were then centrifuged through a layer of 30% percoll to remove debris and dead cells. Spleens were homogenized in HBSS containing HEPES, L-glutamine and pen-strep (HGPG) using frosted slides. For lung homogenate, lungs were minced, homogenized, homogenate resuspended in a total volume of 1 ml PBS, pressed through a 70-mm cell strainer, centrifuged and clarified supernatant collected for analysis.

Antibodies, immunoblotting, detection assays, siRNA knockdowns and flow cytometry. Cells were washed with PBS and lysed with RIPA buffer containing protease inhibitor cocktail (Roche). Cells extracts were analyzed by standard immunoblotting techniques with antibodies to ASC (Enzo Life Science, AL177), procaspase-1 and active caspase-1 (P20) (Cell Signaling, 2225), GFP (Abcam), calpain I (Cell Signaling), p62 (Abcam) and actin (Sigma). Proteins were resolved on a 12 % SDS-polyacrylamide gels and transferred to nitrocellulose membranes. The membrane was blocked for 1h in 5% non-fat dried milk in PBS/Tween 20 (0.1%) and probed with primary antibody overnight at 4°C. After washing with PBS/Tween, the blot was probed with appropriate anti-mouse HRP-conjugated secondary antibody for 1 h at room temperature and stained with SuperSignal West Dura chemiluminescent substrate (Thermo Fisher Scientific). Actin was used as standardization control. For siRNA knockdowns, BMM were transfected by nucleoporation using Nucleofector Reagent Kit Mouse Macrophage (Amaxa/Lonza Biosystems). For murine p62 or Atg5 knockdowns, cells were transfected with siGENOME SMARTpool reagents (Dharmacon):

p62: (GCATTGAAGTGGATATTGA; GACGATGACTGGACCCATT; TCGGAGGATCCCAGTGTGA; CAGCAAGCCGGGTGGGAAT);

Atg5: (CCAAUUGGUUUACUAUUUG; CGAAUUCCAACUUGCUUUA; UUAGUGAGAUAUGGUUUGA; GCAUAAAAGUCAAGUGAUC);

ASC (AUACAUCCCUACUUGGUGA, GCUUAGAGACAUGGGCUUA, GCAACUGCGAGAAGGCUAU, CUGCAAACGACUAAAGAAG);

NLRP3 (GUUCUUCGCUGCUAUGUAC; GCACCCAGGCUGUAACAUU; UGAAGGACCCACAGUGUAA; UCACAUUCCUCUAUGGUAU);

CAPNS1 (GGACAGAUCCAAGUGAACA; GUGGCAGGCUAUAUACAAA; GGAGGGAACAUGAGCUCUA; GGGAACAUGGAUUUCGAUA);

Caspase 1 (GAGGAUUUCUUAACGGAUG, GCACGGGACCUAUGUGAUC, GGUAUACCGUGAAAGUGAA, GUACACGUCUUGCCCUCAU).

Non-targeting siRNA pool (Scramble; used as a control) (UAGCGACUAAACACAUCAA; UAAGGCUAUGAAGAGAUAC; AUGUAUUGGCCUGUAUUAG; AUGAACGUGAAUUGCUCAA).

At 48 h post transfection, cells were stimulated overnight with LPS and IFNγ (1μg/ml and 5ng/ml, respectively) and the supernatants were collected for further analysis. Cells were collected and analyzed for targeted protein expression by immunoblotting as described above. Flow cytometry was carried out on the LSRFortessa or FACSCalibur (BD Biosciences) and data analyzed using FlowJo software (TreeStar).

Quantitative RT PCR. Total RNA was isolated from BMM using RNeasy kit (Qiagen) and cDNA was generated using QuantiTect Reverse Transcription kit (Qiagen). RT-PCR was performed using SYBR Green I QuantiFast SYBR Green Kit (Qiagen) using the following amplification conditions: PCR initial activation step: 95^{O}C-5min; Two-step cycling: Denaturation: 95^{O}C-10 sec; Combined annealing/extension: 60^{O}C-10 sec; Number of cycles 40. The primers for IL-1a: (F) 5'-GCA ACG GGA AGA TTC TGA AG-3'; (R) 5'-TGA CAA ACT TCT GCC TGA CG-3'. The results were analyzed using relative quantification by comparing the ratios of the target gene and the reference housekeeping gene, actin.

Microscopy and image analysis. For confocal microscopy, BMM were stained with mouse anti-GFP (Abcam, 10 μg/ml) to enhance LC3-GFP visualization, rabbit anti-caspase 1 (Santa Cruz Biotechnology), rabbit anti-calpain 1 (Cell Signaling Technology), or hamster anti-IL-1α (eBioscience) followed by secondary antibodies. Pearson's colocalization coefficients were derived using SLIDEBOOK 5.0 (Intelligent Imaging Innovations) applying the SLIDEBOOK 5 default algorithm command 'AND'. All Pearson's coefficients were derived from three independent experiments with five fields or more per experiment, for a total of 15 fields contributing to the cumulative result.

Statistical analysis. Statistical analysis was performed as described in figure legends and graphs generated display the mean (±S.E.) and were obtained using GraphPad Prism software Version 5.03 (GraphPad Software, Inc; San Diego, CA). Survival data in

Figure 1 were analyzed by Kaplan-Meier survival analysis with the Log-Rank method, using SigmaStat version 3.0 (Systat Inc, San Jose, California). The difference between the survival curves was significant with $P<0.01$. All other data were analyzed using ANOVA (KaleidaGraph) or two-tailed unpaired Student's *t*-tests (Prism).

Supplementary figure legends

Figure S1. Lung pathology measures and cells in infected Atg5$^{fl/fl}$ LysM-Cre^{+} and Cre^{-} mice. (A) % area of inflamed lung in histological sections (data, range; n=2). (B) Total lung weight; **p<0.01 (t test, n=5). (C-E) Flow cytometric quantification of CD14^{+}, Ly6G^{+} CD11^{+} (PMN) and CD4 and CD8 cells from infected Atg5$^{fl/fl}$ LysM-Cre^{-} and Cre^{+} mice. Data: mean ±SE; *p<0.05 (t test; n ≥ 3). All materials from mice infected aerogeneously with low dose *M. tuberculosis* H37Rv, 4 weeks postinfection.

Figure S2. Cytokines in the lungs of Atg5$^{fl/fl}$ LysM-Cre^{+} and Cre^{-} mice infected with *M. tuberculosis* H37Rv. (A-G) Multiplex cytokine measurement of IL-17, IFN-γ, TNF-α, IL-4, IL-6, MIP-1β, GM-CSF, and IL-1β as detected by Luminex in lung homogenates of Atg5$^{fl/fl}$ LysM-Cre^{-} and Cre^{+} mice infected with low *M. tuberculosis* dose at weeks 3, 4 and 5 postinfection. IL-17 in panel A represents the combined data from 3 independent cohorts of infections for weeks 3, 4, 5 and 6. Data: mean ±SE, *p<0.05,**p<0.01 (t test; n ≥ 3).

Figure S3. Cytokine and cellular analysis of uninfected Atg5$^{fl/fl}$ LysM-Cre^{+} lungs. (A-E) IL-1α, CXCL1, IL-12p70, IL-1β, and IL-17 levels (ELISA) in lung homogenates of uninfected Atg5$^{fl/fl}$ LysM-Cre^{-} and Atg5$^{fl/fl}$ LysM-Cre^{+} mice. (F, G) Flow cytometric quantification of macrophages per organ tissues in uninfected Atg5$^{fl/fl}$ LysM-Cre^{-} and Cre^{+} mice. (H) Activation state of macrophages measured by surface markers CD1d, MHC II, DEC205 and CD86 in the lungs of uninfected Atg5$^{fl/fl}$ LysM-Cre^{-} (left plots) and Cre^{+} mice (right plots). (I,J) Flow cytometric quantification of neutrophils in the lungs and bone marrow of uninfected Atg5$^{fl/fl}$ LysM-Cre^{-} and Cre^{+} mice. Data, mean ±SE, n≥3, *p<0.05, †>0.05 (t test).

Figure S4. T cell activation state and IL-1α role in T cell IL-17 polarization. (A,B) CD44 and CD25 expression on CD4 T cells from lungs of uninfected Atg5$^{fl/fl}$ LysM-Cre^{-} and Cre^{+} mice. (C-F) Intracellular IL-17A production (day 4; release blocked with monensin) by naïve CD4 T cells polarized in the presence of cytokine cocktails: 5 ng/ml TGF-β and 20 ng/ml IL-6, plus 20 ng/ml IL-1α or 20 ng/ml IL-1β. Dot plot (panel C), levels of IL-17A in unstimulated cells (starting material). Histograms (D,E), IL-17A in naïve CD4 T cells polarized in the presence of TGF-β, IL-6 and IL-1α (panel D) or TGF-β, IL-6 and IL-1β (panel E). (F) Percent of IL-17A^{+} CD4 T cells under respective polarizing conditions. Data: mean ±SE; † p>0.05 (t test; n≥3).

Figure S5. Controls for pharmacological induction of IL-1α hypersecretion phenotype in autophagy-competent macrophages. These experiments were carried out as a controls for effects of pharmacological induction of autophagy on IL-1α

secretion shown in Fig. 5F. IL-1β secretion was examined in autophagy-competent Atg5$^{fl/fl}$ LysM-Cre^{-} BMM and IL-1α secretion was measured in autophagy-deficient Atg5$^{fl/fl}$ LysM-Cre^{+} BMM. (A) IL-1β (ELISA) released from Atg5$^{fl/fl}$ LysM-Cre^{-} BMM (identical activation as in Fig. 5F) treated with (A) 50 mg/ml rapamycin (Rap) and 100 nM Bafilomycin A1 (Baf A1) after 12 h of stimulation. (B) IL-1α (ELISA) released from Atg5$^{fl/fl}$ LysM-Cre^{+} BMM (identical activation as in Fig. 5F) in the presence of (A) 50 mg/ml rapamycin (Rap) and 10 mM 3-MA after 12 h of stimulation. Data: mean ±SE; *, $p<0.05$; † (or no symbol) $p>0.05$ (t test; $n\geq3$).

Figure S6. Analysis of p62, autophagosomes, and caspase 1 as potentially contributing factors to the IL-1 hypersecretion phenotype in Atg5$^{fl/fl}$ LysM-Cre^{+} macrophages. (A) Immunoblot assessment of p62/sequestosome 1 knockdown in BMM. (B) IL-1α release from Atg5$^{fl/fl}$ LysM-Cre^{+} BMM (stimulated with LPS and IFN-γ) subjected to p62/sequestosome 1 knockdown (p62 siRNA) relative to siRNA control (scr, scramble). (C) IL-1α released from LPS and IFN-γ stimulated BMM from p62$^{-/-}$ knockout mice treated with Scr (scrambled control) or Atg5 siRNA. (D) Transcriptional analysis (QTRT PCR) of IL-1α gene expression. Total RNA was isolated from Atg5$^{fl/fl}$ LysM-Cre^{-} and Cre^{+} BMM using RNeasy kit (Qiagen) and cDNA was generated using QuantiTect Reverse Transcription kit (Qiagen). (E) Confocal microcopy analysis of IL-1α colocalization relative to LC3 in GFP-LC3 expressing BMM induced for autophagy by starvation (EBSS) in the presence of bafilomycin A1 for 90 minutes. Scale bar, 5 μM; Pearson's colocalization coefficient for IL-1α vs. LC3. (F) Caspase 1 activation in the absence of autophagy. Atg5$^{fl/fl}$ LysM-Cre^{-} or Cre^{+} BMM cells were starved (EBSS) with or without bafilomycin (BafA1) for 2 or 4 h and subjected to immunoblot analysis; Procasp-1, procaspase 1; Casp-1 p20, processed (activated) caspase 1. (G) Quantification of p20 bands from blots as in A, relative to actin. (H) Atg5$^{fl/fl}$ LysM-Cre^{-} or Cre^{+} BMM were stimulated with LPS overnight and caspase-1 activity was assessed by flow cytometry using the FLICA caspase-1 reagent. Data, mean ±SE; *$p<0.05$, **$p<0.01$ and † $p>0.05$ (t test; $n\geq3$).

Figure S7. Analysis of mitochondrial content, mitochondrial polarization state, calpain levels, and calpain localization relative to autophagic organelles in Atg5$^{fl/fl}$ LysM-Cre^{+} macrophages. (A-C) Flow cytometry analysis of cellular mitochondrial content in Atg5$^{fl/fl}$ LysM-Cre^{-} and Cre^{+} BMM stained with MitoTracker Green. A and B, histograms; C average mean fluorescence intensity (MFI) of MitoTracker Green per cell. (D,E) Polarization state of mitochondria in Atg5$^{fl/fl}$ LysM-Cre^{-} and Cre^{+} BMM. (D), Overlay histogram, MitoTracker Red CMXRos in Atg5$^{fl/fl}$ LysM-Cre^{-} and Cre^{+} BMM. (E), Data and statistical analysis of cumulative results represented in D. (F) Immunoblot analysis of calpain I in unstimulated Atg5$^{fl/fl}$ LysM-Cre^{-} or Cre^{+} BMM and quantification of calpain relative to actin. (G) Calpain does not colocalize with the autophagosomal marker LC3. Confocal microscopy image of endogenous calpain I (Capn1) and immunofluorescently (anti-GFP) labeled GFP-LC3 in BMM from GFP-LC3 knock-in mice. Scale bar, 10 μm. Graph, Pearson's colocalization coefficient (n=3) between calpain I and LC3 (note the negative value). Data, mean ±SE, *$p<0.05$, † $p>0.05$ (t test; $n\geq3$).

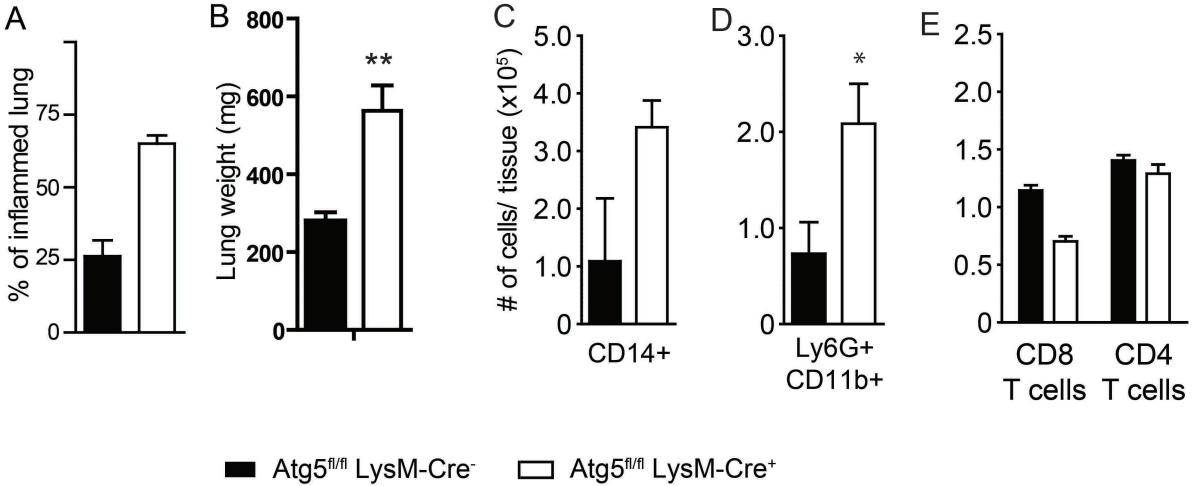
A
% of inflammed lung
0
25
50
75
B
Lung weight (mg)
0
200
400
600
800
**
C
# of cells/ tissue (x10^5)
0
1.0
2.0
3.0
4.0
5.0
CD14+
D
0
1.0
2.0
3.0
*
Ly6G+
CD11b+
E
0
0.5
1.0
1.5
2.0
2.5
CD8
T cells
CD4
T cells
Atg5fl/fl LysM-Cre-
Atg5fl/fl LysM-Cre+

Figure S1

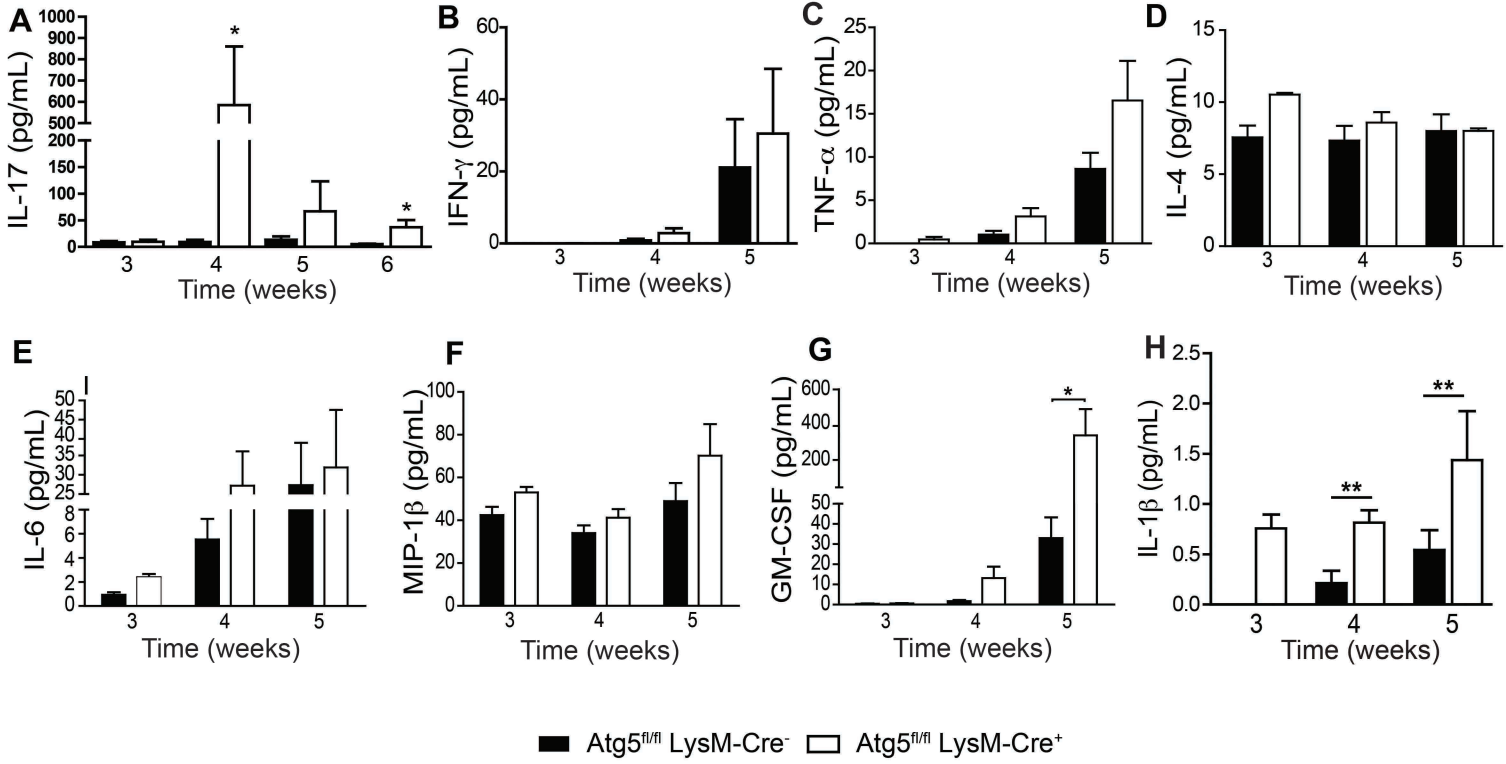
A
IL-17 (pg/mL)
Time (weeks)
B
IFN-γ (pg/mL)
Time (weeks)
C
TNF-α (pg/mL)
Time (weeks)
D
IL-4 (pg/mL)
Time (weeks)
E
IL-6 (pg/mL)
Time (weeks)
F
MIP-1β (pg/mL)
Time (weeks)
G
GM-CSF (pg/mL)
Time (weeks)
H
IL-1β (pg/mL)
Time (weeks)
Atg5fl/fl LysM-Cre-
Atg5fl/fl LysM-Cre+

Figure S2

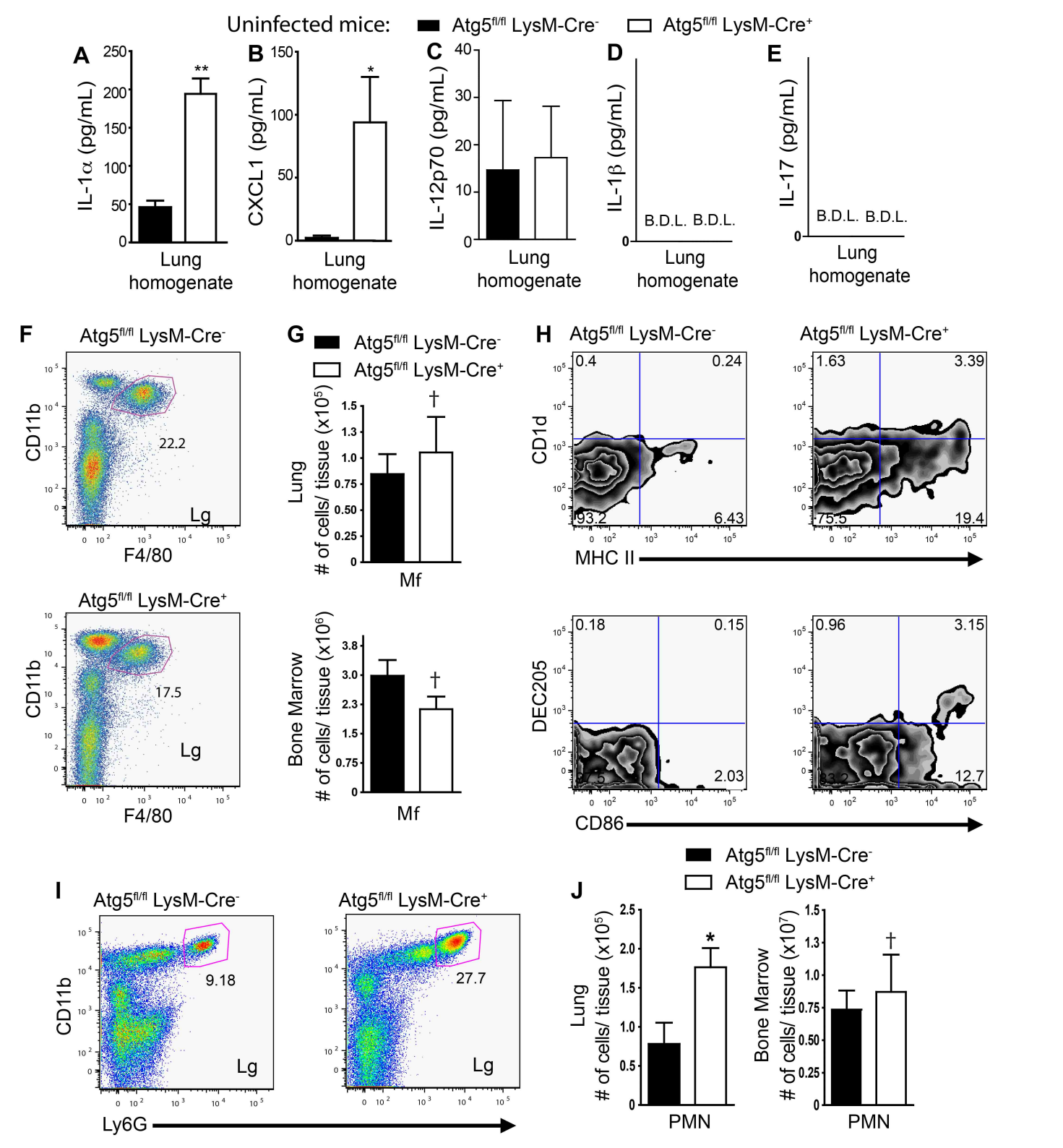
Uninfected mice:
Atg5fl/fl LysM-Cre-
Atg5fl/fl LysM-Cre+
A
IL-1α (pg/mL)
Lung homogenate
B
CXCL1 (pg/mL)
C
IL-12p70 (pg/mL)
D
IL-1β (pg/mL)
B.D.L. B.D.L.
E
IL-17 (pg/mL)
F
CD11b
F4/80
22.2
17.5
Lg
G
# of cells/ tissue (x10^5)
Lung
Mf
# of cells/ tissue (x10^6)
Bone Marrow
H
CD1d
MHC II
0.4
0.24
93.2
6.43
1.63
3.39
75.5
19.4
DEC205
CD86
0.18
0.15
2.03
0.96
3.15
12.7
I
Ly6G
9.18
27.7
J
PMN

Figure S3

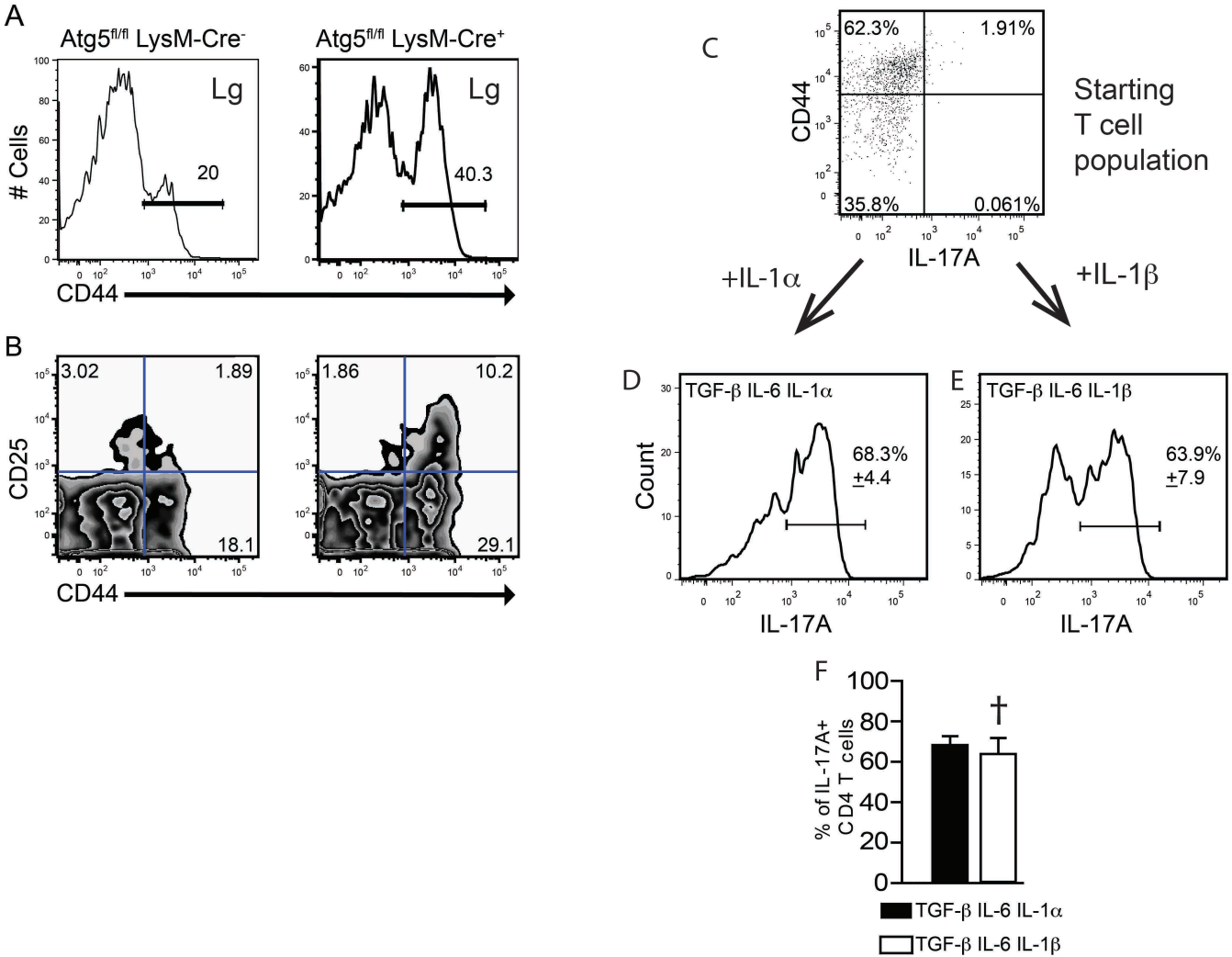
A
Atg5fl/fl LysM-Cre-
Atg5fl/fl LysM-Cre+
Cells
Lg
20
Lg
40.3
CD44
B
3.02
1.89
18.1
1.86
10.2
29.1
CD25
CD44
C
62.3%
1.91%
35.8%
0.061%
CD44
IL-17A
Starting T cell population
+IL-1α
+IL-1β
D
TGF-β IL-6 IL-1α
Count
68.3% ±4.4
IL-17A
E
TGF-β IL-6 IL-1β
63.9% ±7.9
IL-17A
F
% of IL-17A+ CD4 T cells
†
TGF-β IL-6 IL-1α
TGF-β IL-6 IL-1β

Figure S4

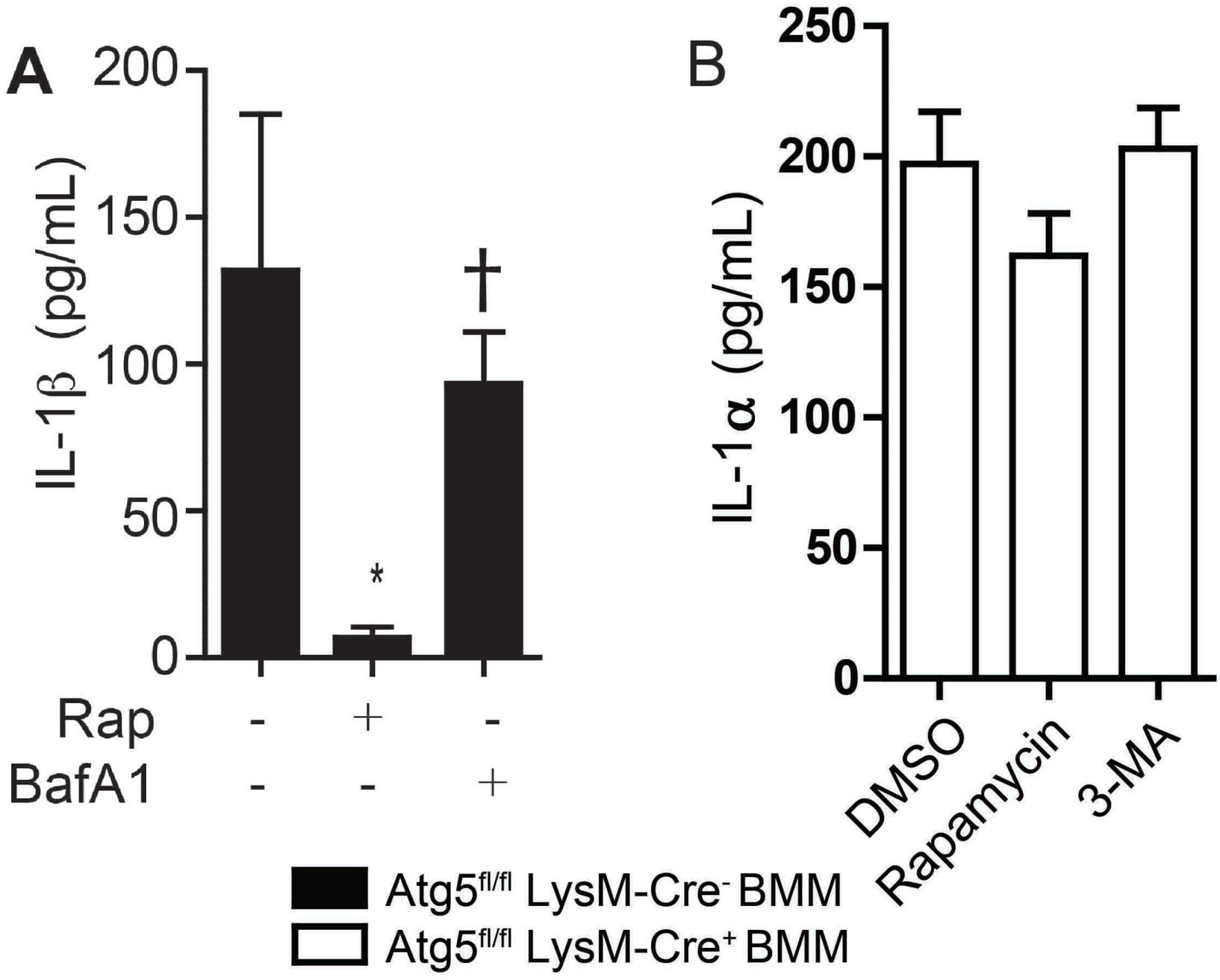
A
200
150
100
50
0
IL-1β (pg/mL)
*
†
Rap
-
+
-
BafA1
-
-
+
B
250
200
150
100
50
0
IL-1α (pg/mL)
DMSO
Rapamycin
3-MA
Atg5fl/fl LysM-Cre- BMM
Atg5fl/fl LysM-Cre+ BMM

Figure S5

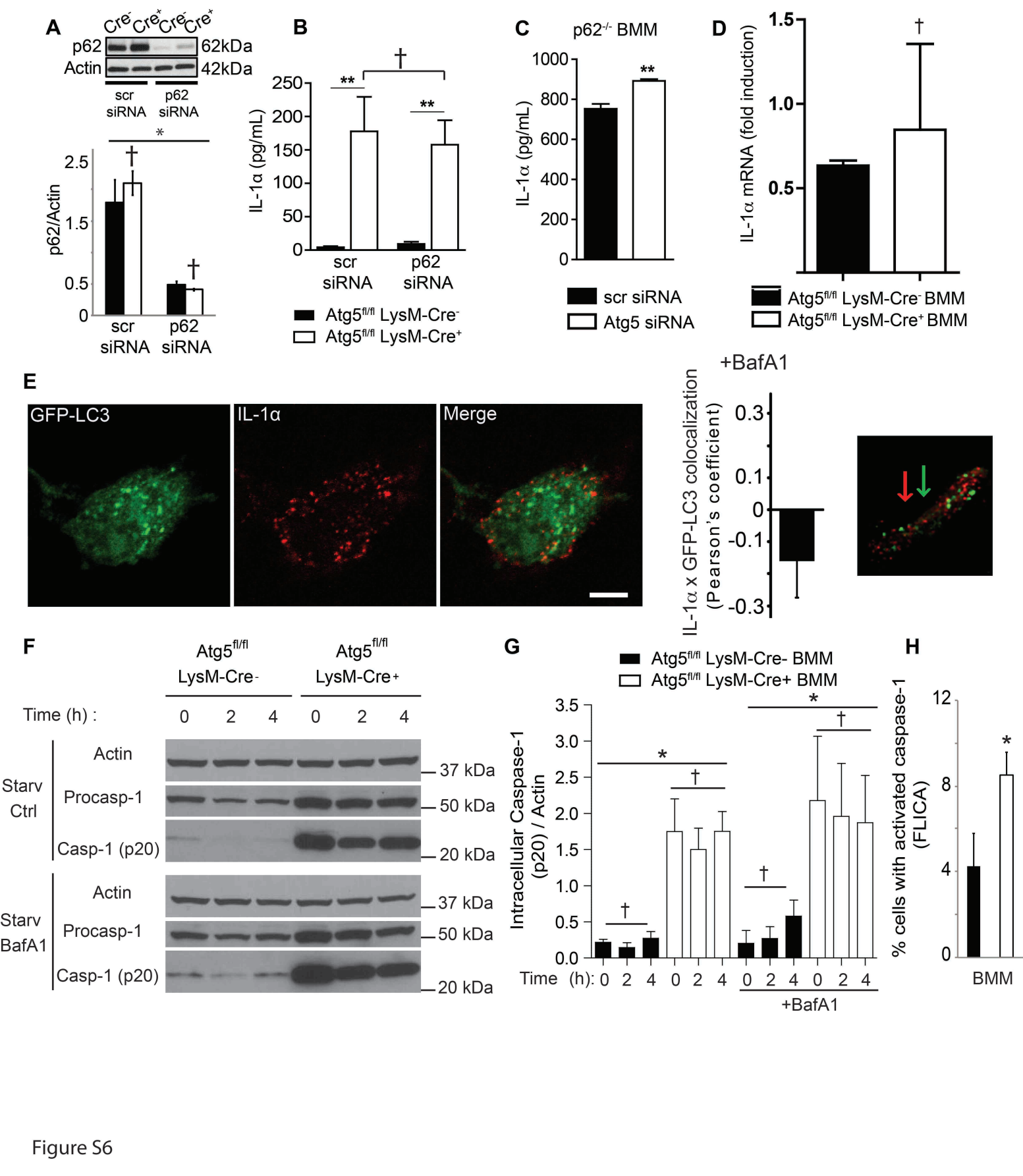
A
Cre- Cre+ Cre- Cre+
p62
Actin
62kDa
42kDa
scr siRNA
p62 siRNA
p62/Actin
scr siRNA
p62 siRNA
B
IL-1α (pg/mL)
scr siRNA
p62 siRNA
Atg5fl/fl LysM-Cre-
Atg5fl/fl LysM-Cre+
C
p62-/- BMM
IL-1α (pg/mL)
scr siRNA
Atg5 siRNA
D
IL-1α mRNA (fold induction)
Atg5fl/fl LysM-Cre- BMM
Atg5fl/fl LysM-Cre+ BMM
E
GFP-LC3
IL-1α
Merge
+BafA1
IL-1α x GFP-LC3 colocalization (Pearson's coefficient)
F
Atg5fl/fl LysM-Cre-
Atg5fl/fl LysM-Cre+
Time (h) :
Starv Ctrl
Actin
Procasp-1
Casp-1 (p20)
Starv BafA1
37 kDa
50 kDa
20 kDa
G
Atg5fl/fl LysM-Cre- BMM
Atg5fl/fl LysM-Cre+ BMM
Intracellular Caspase-1 (p20) / Actin
Time (h):
+BafA1
H
% cells with activated caspase-1 (FLICA)
BMM

Figure S6

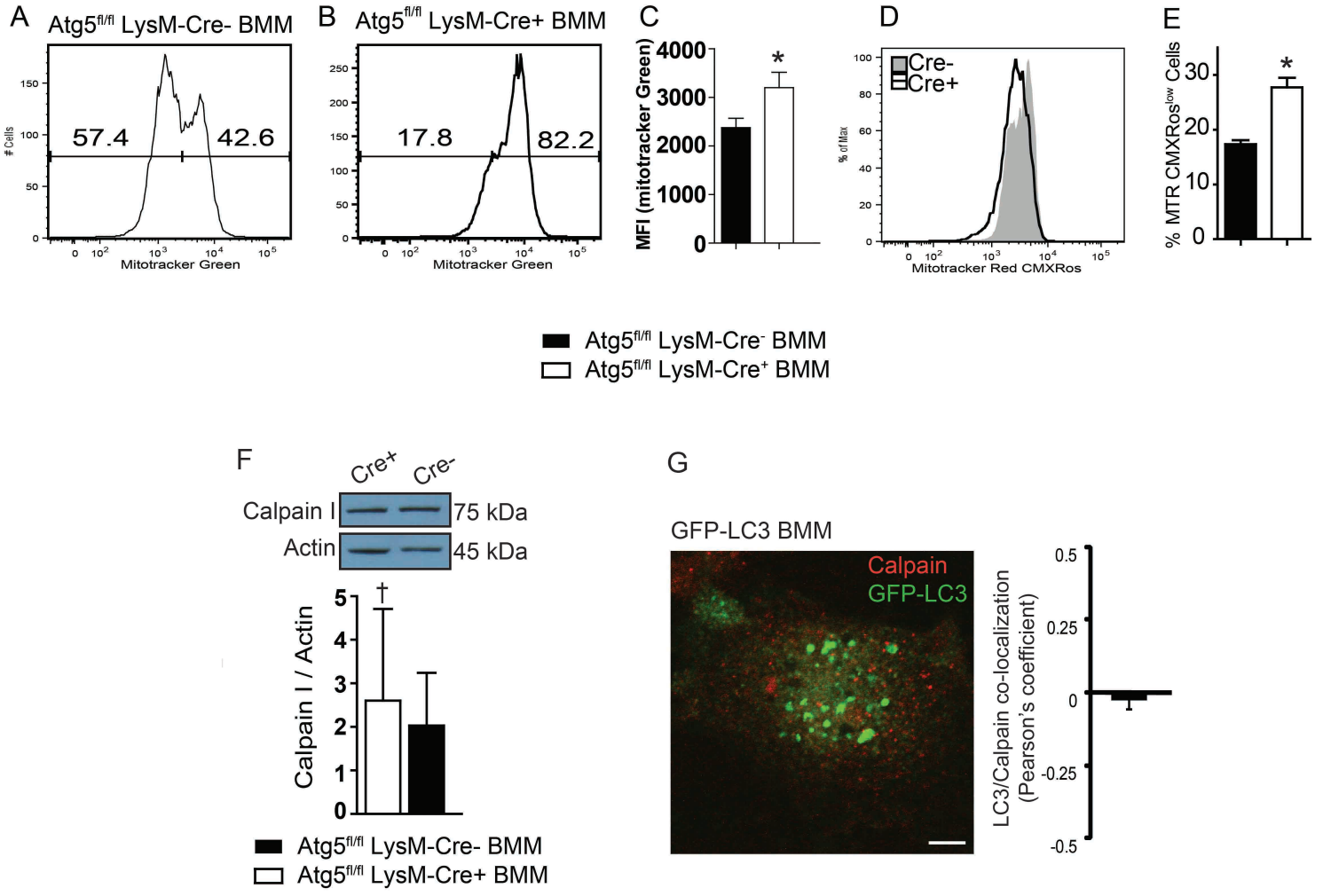
A
Atg5fl/fl LysM-Cre- BMM
57.4
42.6
Cells
Mitotracker Green
B
Atg5fl/fl LysM-Cre+ BMM
17.8
82.2
Mitotracker Green
C
MFI (mitotracker Green)
4000
3000
2000
1000
0
*
D
Cre-
Cre+
% of Max
Mitotracker Red CMXRos
E
% MTR CMXRoslow Cells
30
20
10
0
*
Atg5fl/fl LysM-Cre- BMM
Atg5fl/fl LysM-Cre+ BMM
F
Cre+
Cre-
Calpain I
75 kDa
Actin
45 kDa
Calpain I / Actin
5
4
3
2
1
0
†
Atg5fl/fl LysM-Cre- BMM
Atg5fl/fl LysM-Cre+ BMM
G
GFP-LC3 BMM
Calpain
GFP-LC3
LC3/Calpain co-localization
(Pearson's coefficient)
0.5
0.25
0
-0.25
-0.5

Figure S7